New results from EBW emission experiment on COMPASS

J. Preinhaelter[1], J. Zajac[1], J. Urban[1,2], V. Fuchs[1], M. Aftanas[1], P. Bílková[1], P. Böhm[1], S. Nanobashvili[3], V. Weinzettl [1], F. Žáček[1]

[1] *Institute of Plasma Physics AS CR, v.v.i., Association EURATOM/IPP.CR, Prague, Czech Republic*

[2] *CEA, IRFM, F-13108 Saint Paul-lez-Durance, France*

[3] *Andronikashvili Institute of Physics, Tamarashvili St. 6, 0177 Tbilisi, Georgia*

Abstract. COMPASS tokamak shots with low magnetic field produce overdense plasma during extended current flat-top phase. The first harmonic is completely cut off for O and X-mode electron cyclotron emission (ECE) and so the emission caused by the electron Bernstein waves (EBWs) propagating obliquely with respect to the magnetic field and undergoing so cold EBW-X-O conversion process can be observed. We employ a horn antenna system with a toroidally and poloidally steered ellipsoidal mirror detecting alternatively one from two linearly orthogonally polarized waves using a 16-channel radiometer, operating in the 26.5 – 40 GHz band [1]. The whole apparatus including the vacuum window was absolutely calibrated; therefore, it measures directly the radiant temperature. We perform an angular scan of the EBW emission during a set of comparable shots in order to determine the optimum antenna direction. We study the time development of the temperature profiles deduced from the EBW signal. Results are compared with simulations using AMR and ACCOME codes. To verify the resulting temperature profiles we also compare with Thomson scattering data for the same shots.

Introduction. Electron cyclotron emission is an experimental technique successfully used for non-perturbative detection of plasma parameters, specifically the electron plasma temperature. In a dense plasma, the plasma cutoff exists near the boundary and the direct detection of O or X modes is impossible. In this case, the electron Bernstein waves excited at the electron cyclotron resonances and linearly converted to the X-mode in the upper hybrid resonance (UHR) region can be emitted either directly as X-modes (EBW-X tunneling) or after the transmission through the plasma resonance region and the X-O conversion as O-modes (EBW-X-O conversion), as reviewed in [2]. An overdense plasma typically arises in the COMPASS [3] tokamak at low magnetic fields (B_t~1 T) and at the line averaged density above $2x10^{19}m^{-3}$ (see Fig. 1). COMPASS is a compact (R = 0.56 m, a = 0.23 m, $I_p \leq 350$ kA, B_t = 0.8 – 2.1 T) tokamak, originally residing at Culham laboratory, CCFE, and now reinstalled at IPP Prague. At Culham, the EBW emission from COMPASS was measured in the 60 GHz range in

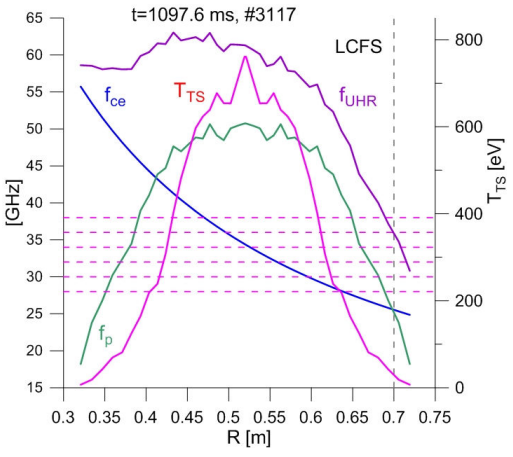

Fig. 1. Radial profiles of the electron cyclotron f_{ce}, plasma f_p and upper hybrid f_{UHR} frequencies and the electron temperature T_{TS} in the typical COMPASS discharge with circular cross-section. The density and temperature are derived from Thomson scattering measurement. Plasma is shifted radially toward the HFS by about 4cm from vessel center at R=0.56m. B_t=1.14 T.

the midplane perpendicularly to the magnetic field and weak EBW-X tunneling was observed [4].

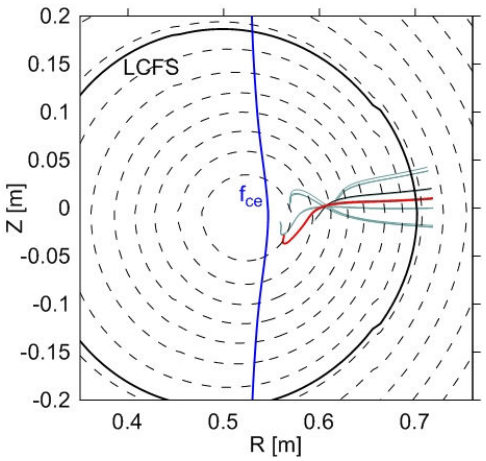

Fig. 2 EBW rays in COMPASS tokamak plasma. The incident beam has the frequency f=32.875 GHz and the incident angels $\alpha_{tor} = 31^o$, $\alpha_{pol} = 2^o$.

We present the results of detection of EBW emission. The 1st harmonic radiation is detected, after the EBW-X-O conversion, by a recently installed system consisting of an angularly steered ellipsoidal mirror, a horn antenna and a Ka-band radiometer. From Fig. 1, it follows that the EBW emission can be observed for the whole range of available frequencies.

EBW emission modeling. To obtain a deeper insight into the EBW emission from COMPASS we perform simulations with our AMR (Antenna, Mode-conversion, Ray-tracing) code [5]. For magnetic surface equilibrium reconstruction, we use the code ACCOME [6] for the given circular plasma shape of the respective shots. The temperature and density profiles are reconstructed by the mapping of the measured Thomson scattering values on the vertical chord to the magnetic surfaces. Because of the uncertainty in many parameters, detailed comparison of the EBW experiment with the simulation is not easy and we cannot reach the same excellent match as in the case of our simulation for MAST and NSTX [7].

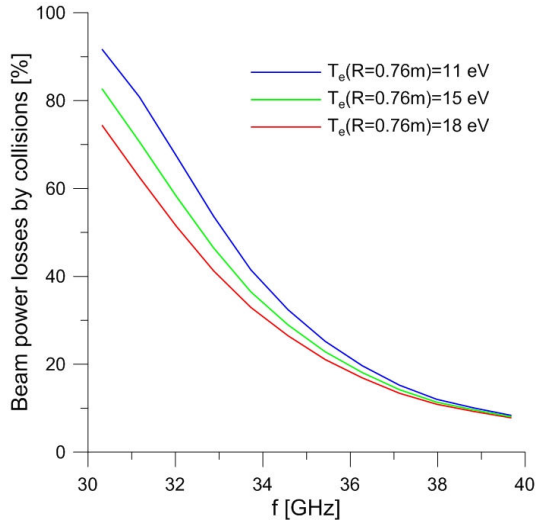

Fig. 3. Frequency dependence of power absorbed by collisions of EBW beam of in the upper hybrid conversion region. $\alpha_{tor} = 31^o$, $\alpha_{pol} = 2^o$.

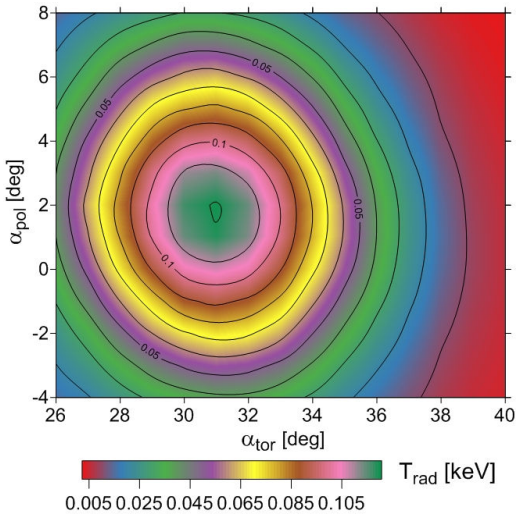

Fig. 4. Simulated dependence of T_{rad} on the angles of the detected beam for $f = 32.875$ GHz. #3117, $T_e = 18$ eV and $Z_{eff} = 3$ at LCFS.

In Fig. 2 we see the poloidal cross-section of COMPASS with circular magnetic surfaces and set of EBW rays representing outgoing beam originated at the first cyclotron harmonics and ending near the UHR. If UHR is situated out of the last closed flux surface (LCFS), as it is for COMPASS, the electron ion collisions are responsible for EBW damping [8]. In Fig. 3 we present the EBW power losses caused by collisions. If we disregard the collisional damping, the EBW is at UHR fully converted to the X mode, which is converted to the O-mode in the plasma resonance region (PR). The X-O conversion is strongly dependent on the angle ϑ_{tor} between the incident wave-vector and the total magnetic field and on the angle ϑ_{pol} between the wave-vector and the plane given by the magnetic field and the density gradient (all

quantities evaluated at the PR). The evanescent region in the PR disappears if $\vartheta_{tor} = \cos^{-1}\sqrt{(f_{ce}/(f+f_{ce}))}$ and $\vartheta_{pol} = 0$. The angular dependence of transmission coefficient through the PR was firstly derived in [9]. The approximate optimum angles in the antenna system are: $\alpha_{pol} = \sin^{-1}(N_{\|}B_{\varphi}/B)$ and $\alpha_{tor} = \sin^{-1}(R_{pr}\sin(90^o+\vartheta_{tor})/R_m)$, where $N_{\|} = \cos(\vartheta_{tor})$, R_m and R_{pr} are the radial coordinate of the mirror center and the plasma resonance, respectively. Because we detect linearly polarized wave ($E \| B_0$) the transmission for the optimum ray is only 60% (the oblique O wave is elliptically polarized). The simulated angular dependence of T_{rad} on α_{tor} and α_{pol} is given in Fig. 4. Due to the combined effects of the collisional damping of EBW, the conversion efficiency of X-O conversion process and the beam angular divergence, the radiating temperature detected by the antenna can be only 120 eV at the optimum ($\alpha_{tor} = 31^o$, $\alpha_{pol} = 2^o$), which is substantially lower that the TS value (~650 eV).

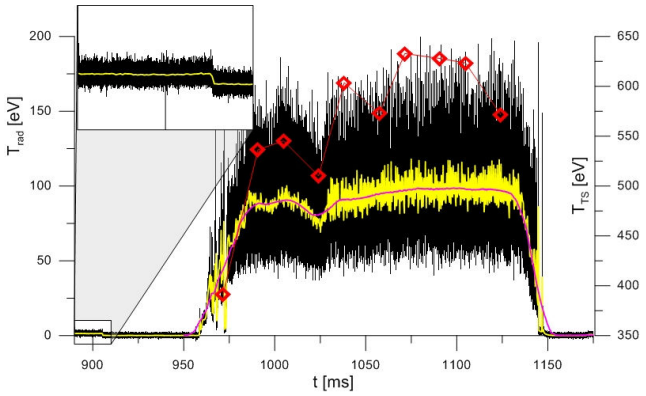

Fig. 5. Time development of the signal from the plasma center (f=32.875 GHz, #3127, α_{tor}=28° and α_{pol}=0°). Diamonds correspond to the Thomson scattering temperature T_{TS}.

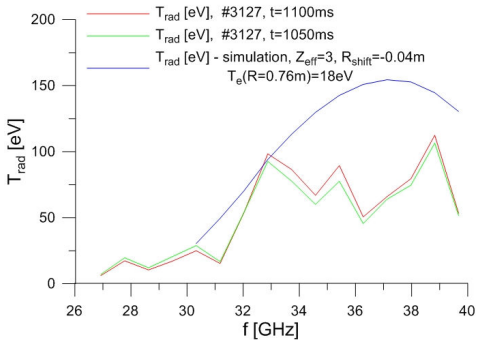

Fig. 6. EBW emission spectrum detected on COMPASS. α_{tor}=28°, α_{pol}=0°.

Results of detections of EBW emission. Presently, only circular discharges are reliably reproducible on COMPASS with a current flat top I_p=130 kA. If the line averaged density is higher then $2\text{x}10^{19}$ m^{-3}, such discharges are practically free of runaway electrons (detected by the X-ray signal [10]) and produce standard EBW signals with constant intensity lasting for more than 100 ms.

In Fig. 5 we present the detailed picture of the time development of the signal f=32.875 GHz corresponding to the emission from the plasma center. We see that after the initial transition phenomenon it develops a plateau of a constant emission for about 100 ms. The single averaged signal (running average with the window width equal to 351 and 1/500 sampling, yellow line) is used to highlight the noise generator (see the inset) which is used for a shot to shot calibration. To compare the highly noisy signals, we use the double averaged (additional averaging with the window width 55) smooth curve seen (magenta in Fig 5).

To find the optimum, i.e. the most intense signal corresponding to the full transmission waves through the plasma resonance region, we perform an extended scan of the antenna angles. In Figs. 7 and 8 we present a selection of representative shots (the angels can be changed only between the shots). The experimental optimum of T_{rad} is reached at $\alpha_{tor} \sim 30^o$ and $\alpha_{pol} \sim -2^o$, which is in a good agreement with the simulation (see Fig. 4). (The magnetic field and the plasma current are directed to the left if we stand in front of tokamak, both opposite than those used in the simulations). The angular dependence of T_{rad} is much weaker than predicted

by the simulation (see Fig. 4) which suggest that the tokamak chamber is filled by the diffracted radiation.

The frequency profile of T_{rad} is given in Fig. 6. It can be used to reconstruct the temporal behavior of the radial electron temperature profile. We see that the radiative temperature has a local maximum at 33 GHz corresponding to the emission from the plasma center. The low frequency part of the spectrum is faint but the high frequency part shines intensively. The minimum at 36 GHz is missing in the simulated spectrum. One possible explanation is that the magnetic surfaces on the high field side are deformed and the first harmonic is open. Hence, the signal at 38 GHz might correspond to the direct ECE, which is not collisionally damped in UHR.

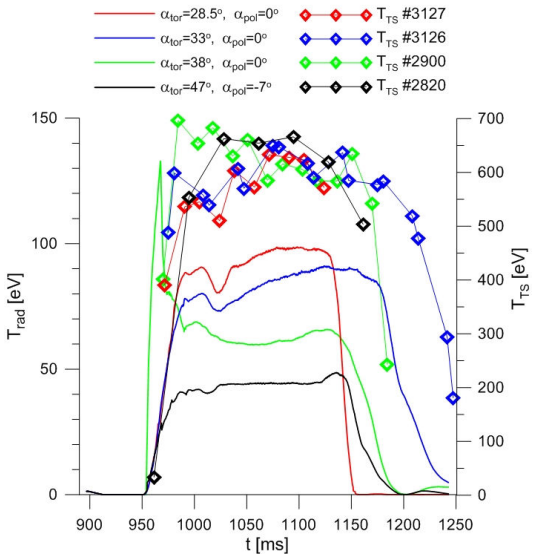

Fig. 7. Dependence of the time traces of the 32.875 GHz signals (full lines) on the incident angles. Diamonds correspond to the Thomson scattering temperature.

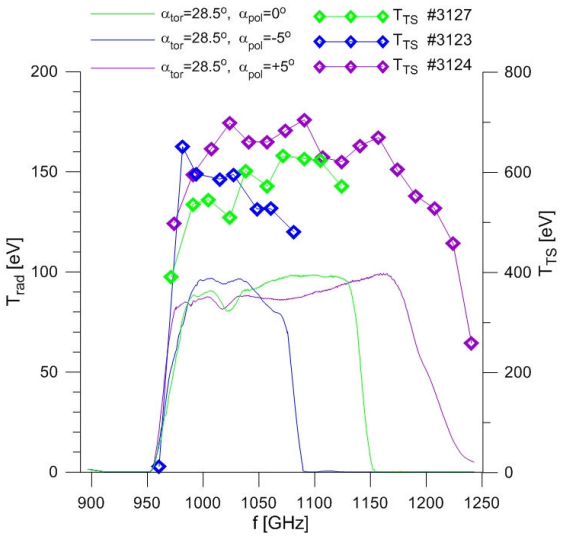

Fig. 8. Dependence of the time traces of the 32.875 GHz signals (full lines) on the poloidal angles.

Acknowledgements. Work is supported by Czech Science Foundation grant 202/08/0419, by MSMT projects 7G10072, and LM2011021, by EURATOM, by EFDA, by AS CR project 0Z-20430508. and by SRNSF (Georgia) grant FR/443/6-140/11.

References

[1] J.Zajac, et al., Rev. Sci. Instrum. **81**, 10D911 (2010), J.Zajac, et al., Rev. Sci. Instrum. (2012) to be published
[2] H. Laqua, Plasma Phys. Control. Fusion **49** R1–R42 (2007)
[3] R. Panek, et al., Czechoslovak Journal of Physics **56B**, B125-B137 (2006).
[4] V. Shevchenko, et al.,AIP **694** 359 (2003)
[5] J. Urban, et al., J. Plasma Fusion Res. Ser. **8** 1153 (2009)
[6] K. Tani, M. Azumi, R. S. J. Devoto, J. Comp. Phys., **98** 1992) 332.
[7] J. Preinhaelter, et al., AIP **787** 349 (2005)
[8] S. J. Diem, et al., Phys. Rev. Lett. .**103** 015002 (2009)
[9] J. Preinhaelter and V. Kopecky, Journal of Plasma Physics **10** 1 (1973); see also J. Preinhaelter, Czechoslovak Journal of Physics **25** 39 (1975)
[10] V.Weinzettl, et al., Fus. Eng. Des. 86 1227 (2011)